Time-Varying Harmonic Distortion Estimation Using PLL Based Filter Bank and Multirate Processing

J. R. Carvalho, C. A. Duque, *Member*, *IEEE*, M. V. Ribeiro, *Member*, *IEEE*, A. S. Cerqueira, T.L. Baldwin, *Senior*, *IEEE*, and P. F. Ribeiro, *Fellow*, *IEEE*

***Abstract*--This paper describes a PLL (*Phase-Locked Loop*) based harmonic estimation system which makes use of an analysis filter bank and multirate processing. The filter bank is composed of bandpass adaptive filter. The initial center frequency of each filter is purposely chosen equal to harmonic frequencies. However, the adaptation makes possible tracking time-varying frequencies as well as inter-harmonic components. A down-sampler device follows the filtering stage reducing the computational burden, specially, because an undersampling operation is realized. Finally, the last stage is composed by a PLL estimator which provides estimates for amplitude, phase and the apparent frequency of input signal. The true values of frequencies are obtained from the apparent frequency using simple algebraic equations. Simulations show that this approach is precise and faster than other PLL structures.**

***Index Terms*--PLL, Time-varying harmonic estimation, multirate signal processing.**

I. INTRODUCTION

WITH the increased application of power electronics, controllers, motor drives, inverters, and FACTS devices in modern power systems, distortions in line voltage and current have been increasing significantly. These distortions have affected the power quality of the power system and to maintain it under control the monitoring of harmonic and inter-harmonic distortion is an important issue [1]-[3].

The DFT (*Discrete Fourier Transform*) is a suitable approach for estimate the spectral content of a stationary signal, but it loses accuracy under time varying conditions [4] and, as a result, other algorithms must be used. The Short Time Fourier Transform (STFT) can partly deal with time varying conditions but it has the limitation of fixed window width chosen a priori and this imposes limitation for the analysis of low-frequency and high-frequency non-stationary signal at the same time [5].

This work was supported in part by CNPq under Grant 550178/2005-8 and CAPES, all from Brazil. Janison R. Carvalho, Carlos A. Duque, Moisés V. Ribeiro and Augusto S. Cerqueira are with Electrical Engineering Dept., UFJF, Juiz de Fora MG, Brazil, 36.036-330. Phone: (+55) 32-32293442, email: janison@labsel.ufjf.br, carlos.duque@ufjf.edu.br, mribeiro@ieee.org, augusto.santiago@ufjf.edu.br.

Paulo F. Ribeiro is CAPS/FSU and Calvin College (e-mail: pfribeiro@ieee.org, Thomas L. Badwin is with CAPS / FSU (e-mail: tom.baldwin@ieee.org)

The IEC standard drafts [6] have specified signal processing recommendations and definitions for harmonic and inter-harmonic measurement. These recommendations utilize DFT over a rectangular window of exactly 12 cycles for 60 Hz (10 cycles for 50 Hz) and frequency resolution of 5 Hz. However, different authors [7], [8] have shown that the detection and measurement of inter-harmonics, with acceptable accuracy, is difficult to obtain using the IEC specification.

Unlike the previous methods, that follow the IEC standard, others techniques based on Kalman filter, adaptive notch filter or PLL approaches have been applying in harmonic and inter-harmonic estimation. The main disadvantage of Kalman filter based harmonics estimation is the higher order model required to estimate several components.

In [3], the EPLL (*Enhanced Phase-Locked Loop*) [1] is used as the basic structure for harmonic and inter-harmonic estimation, and several of such sections are arranged together. Each one is adjusted to estimate a single sinusoid waveform. The convergence takes about 18 cycles, but it can take more than 100 cycles for higher harmonic frequencies, mostly if there is a fundamental frequency deviation.

In [9], a new multi-rate filter bank structure for harmonic and inter-harmonic extraction is presented. The method uses EPLL as estimation tool in combination with sharp bandpass filters and down-sampler devices. As a result, an enhanced and low computational complexity method for parameters estimation of time-varying frequency signals is attained.

This work presents a new version of the proposed method in [9]. This new version uses the concept of apparent frequency and the undersampling principle. These concepts are correlated with each other. In addition to reducing the computation effort of the overall estimator, they guarantee that robust structures can be implemented in fixed point processors.

This paper is organized as follows: Section II presents some concepts about digital filter bank. Section III describes the multirate processing, the concepts of undersampling and apparent frequency. Section IV describes the proposed structure and the recursive equations of the PLL method [1]. Section V presents numerical results. Finally, in Section VI, some concluding remarks are stated.

II. DIGITAL FILTER BANK

A digital filter bank [10] is a collection of digital bandpass filters with either a common input (the analysis bank) or a summed output (the synthesis bank). The object of discussion in this section is the analysis bank.

The analysis filter bank decomposes the input signal $x[n]$ into a set of M subband signals $y_1[n]$, $y_2[n]$,…, $y_M[n]$, each one occupying a portion of the original frequency band. Fig. 1 shows a typical analysis filter bank.

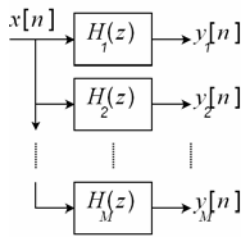

Fig. 1. A typical analysis filter bank

In this work, the filter bank differs from traditional filter banks found in the literature [10]. Specially, bandpass filters split the input signal into the spectrum. These filters are conventional parametric bandpass filters [11] given by

$$H(z)=\frac{1-\alpha}{2}\cdot\frac{1-z^{-2}}{1-\beta(1+\alpha)z^{-1}+\alpha z^{-2}} \qquad (1)$$

The above transfer function has a narrow bandwitdh, when the poles are a pair of complex conjugate near the unit circle. The parameter α controls this proximity defining the 3dB-bandwith of the filter. The maximum magnitude value of (1) occurs at discrete frequency ω_0 which is related with β, by the expression $\beta=\cos(\omega_0)$. The magnitude response of (1) is plotted in Fig. 2 for the band pass centered at fundamental frequency (60 Hz) and some of its harmonics. Solid lines are for second order filter of (1) while dashed lines show the response for a cascade structure of two second order filters.

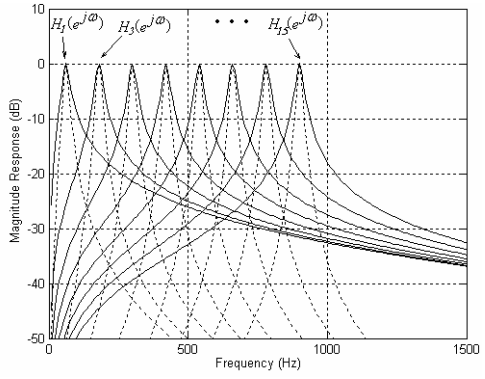

Fig. 2. Magnitude Responses of the Bandpass Filters of the Analysis Bank

Although the parameter α near unit produces a sharper magnitude response, it increases the transient response time. This fact is very important because the converge time of the estimator is proportional to the duration of the transient period. For example, using (1) with α=0.98 and an input signal of 60Hz with 128 points per cycle, the transient virtually decays at about four cycles.

III. MULTIRATE PROCESSING

The two basic components in sampling rate modification are: the down-sampler, to reduce the sampling rate; and the up-sampler, to increase the sampling rate [11]. The block diagram representation of these two components is shown in Fig. 3. The down-sampler will be described in this section.

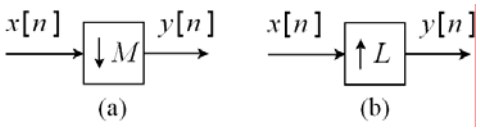

Fig. 3. (a) Block diagram representation of a down-sampler. (b) Block diagram representation of an up-sampler

A down-sampler with a down-sampling factor M, where M is a positive integer, creates an output sequence $y[n]$ with a sampling rate M times smaller than the sampling rate of the input sequence $x[n]$. In other words, this device keeps every Mth sample of the input signal, removing the others M-1.

The input-output relationship can be written as

$$y[n]=x[nM] \qquad (2)$$

In frequency domain it can be shown that

$$Y(e^{j\omega})=\frac{1}{M}\sum_{k=0}^{M-1}X(e^{j(\omega-2\pi k)/M}) \qquad (3)$$

Equation (3) implies that the DTFT (*Discrete-Time Fourier Transform*) of the down-sampled output signal $y[n]$ is a sum of M uniformly shifted and stretched versions of DTFT of input $x[n]$, scaled by a factor $1/M$. It can be shown that aliasing due to down-sample operation is absent if and only if the input signal is band-limited to $\pm\pi/M$.

Fig. 4 illustrates an example of down-sample effect in the frequency domain by direct application of (3). The solid curve is the spectrum of the input signal. With M=4, the dashed line is the shifted and stretched spectrum of output signal. It can be seen that the peak value has been moved from 0.1563 radians to 0.6250 radians, while the frequency remains equal to 300 Hz.

An alternative and simple interpretation of (3) can be done assuming a single sinusoidal signal at input. Fig. 5(a) shows a circle where the sinusoidal component of frequency f is correctly placed with an angle $\theta=(f/f_N)\cdot\pi$ radians, where f_N is the Nyquist frequency. After down sampling with a factor M, the input, exhibits a new angle position: $\theta_M=M\theta$, as shown in Fig. 5(b).

There are some singularities to be considered here. Firstly, if $\theta_M<\pi$ the output has the same frequency in Hertz as its input, like in Fig. 4. Secondly, if $\pi<\theta_M<2\pi$ the output was obtained by undersampling [11] the input, what means that sampling theorem was not attended. In this case it is necessary to find the value of the output frequency f', called the apparent

frequency, by analyzing the angle 2π-$M\theta$ and the new Nyquist frequency. This is illustrated in Fig. 5(b). Finally, if θ_M>2π, an undersampling was performed again and the full revolutions must be discounted. In this case it is necessary to find the value of the apparent frequency f' by analyzing the angle $M\theta$-2π and the new Nyquist frequency.

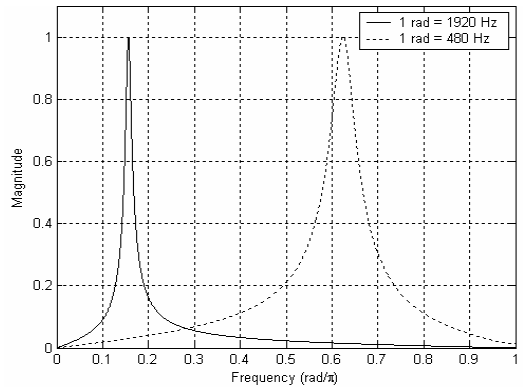

Fig. 4. Effect of down-sample operation in frequency domain

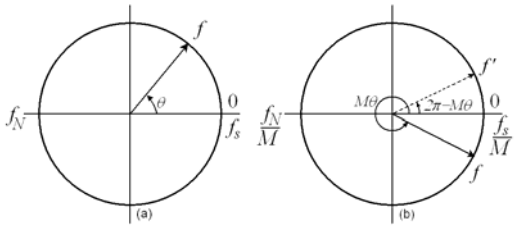

Fig. 5. Alternative interpretation of down-sample effect in a single sinusoidal signal (a) Original position of component with frequency f. (b) Position of component after down-sample operator

IV. PROPOSED STRUCTURE

Fig. 6 shows the proposed structure to harmonic estimation. Fifteen bandpass filters compose the filter bank., Each bandpass filter has been previously designed with an initial central frequencies at the fundamental power frequency or one of the harmonic frequencies. The input signal $x[n]$ has ideally a frequency of f_0=60 Hz and the sampling rate used is f_S=128·f_0.

After filtering stage, the down-sampler device reduces the sampling rate, performing the undersampling of $y_k[n]$ for k=5,6,…,15, according Table I. Here we point another difference between this filter bank structure and that commonly found in literature: the down-sampling factors are not equals. There are many possible values of M_k. Table I shows typical values used for simulation and their effects in changing frequency of input signal $y_k[n]$.

We can apply this understand to a row of frequencys given in Table I. For example, the 9th harmonic sequence $y_9[n]$ passed through a down-sampler device with factor M_9=16 results in an output sequence $v_9[n]$ with apparent frequency equals to 60 Hz.

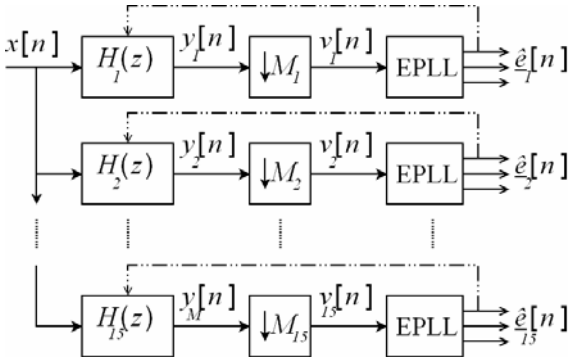

Fig. 6. Proposed structure for harmonic estimation

TABLE I
TYPICAL VALUES FOR DOWN-SAMPLING FACTOR AND ITS EFFECTS IN CHANGING FREQUENCY OF INPUT SIGNAL

k	M_k	Frequency (Hz)		k	M_k	Frequency (Hz)	
		$y_k[n]$	$v_k[n]$			$y_k[n]$	$v_k[n]$
1	16	60	60	**9**	16	540	60
2	8	120	120	**10**	11	600	98.18
3	16	180	180	**11**	16	660	180
4	12	240	240	**12**	12	720	80
5	16	300	180	**13**	16	780	180
6	14	360	188.57	**14**	15	840	184
7	16	420	60	**15**	16	900	60
8	14	480	68.57	-	-	-	-

Finally, the last stage is the estimator stage. This is composed by the Enhanced-PLL (EPLL) system [1], which is responsible to extract three parameters from its input signal $v_k[n]$. These parameters are the magnitude, the frequency (apparent frequency) and the total phase, that is

$$\underline{\hat{e}}_k[n] = \left[\hat{A}_k[n] \quad \hat{\omega}_k[n] \quad \hat{\phi}_k[n]\right]^T \tag{4}$$

The EPLL discrete-time recursive equations are:

$$\begin{aligned} \hat{A}_k[n+1] &= \hat{A}_k[n] + \mu_1 e_k[n]\sin\left(\hat{\phi}_k[n]\right) \\ \hat{\omega}_k[n+1] &= \hat{\omega}_k[n] + \mu_2 e_k[n]\cos\left(\hat{\phi}_k[n]\right) \\ \hat{\phi}_k[n+1] &= \hat{\phi}_k[n] + T_S\hat{\omega}_k[n] + \mu_3 e[n]\cos\left(\hat{\phi}_k[n]\right) \end{aligned} \tag{5}$$

where μ_1, μ_2 and μ_3 are constants that determine de speed of convergence, T_S is the sampling period and $e_k[n]$ is the error signal given by

$$e_k[n] = v_k[n] - \hat{A}_k[n]\sin(\hat{\phi}_k[n]) \tag{6}$$

From Fig. 6 it can be seen that the estimated frequency of each EPLL block is used to update its respective bandpass filter. There are many strategies to do this and here we chose to update always when the index time n is a multiple of a constant J.

V. SIMULATIONS RESULTS

This section presents the performance of proposed method under a variety of conditions applied to the input signal.

Simulations results are also compared with those presented in references[1]-[3]. A cascade structure of two filters (1) was used with α=0.98. The EPLL constants μ_1, μ_2 and μ_3 are $300T_S$, $500T_S$ and $6T_S$, respectively.

A. Presence of harmonics

This case shows the behavior of the system when the input is composed by the fundamental with odd harmonics

$$x(t)=V_M \sin(\omega_0 t)+\frac{1}{3}V_M \sin(3\omega_0 t)+\frac{1}{5}V_M \sin(5\omega_0 t) + \frac{1}{7}V_M \sin(7\omega_0 t)+\frac{1}{9}V_M \sin(9\omega_0 t)+\frac{1}{11}V_M \sin(11\omega_0 t) + \frac{1}{13}V_M \sin(13\omega_0 t)+\frac{1}{15}V_M \sin(15\omega_0 t) \quad (7)$$

Fig. 7 shows results of the amplitude estimation. Unlike DFT methods, in which steady-state occurs in one cycle, Fig. 7(a) shows that steady-state is approximately reached in 5 cycles. Although slower than DFT, this result is faster than the one related in [3]. This is mostly due to the use of the bandpass filters, which permits to increase gains μ_1, μ_2 and μ_3 without increasing the steady-state error. Fig. 7(b) shows a zoom in the estimation of harmonics components.

B. Presence of additive White Gaussian Noise

In this case it is evaluated the behavior of the system when the input signal is corrupted by a zero-mean White Gaussian additive noise, $n(t)$, as

$$x(t)=V_M \sin(\omega_0 t)+n(t) \quad (8)$$

Fig. 8 shows results of amplitude estimation for input signal of (8) and a signal-to-noise ratio (SNR) equal to 15dB. The solid line is the output of the EPLL block and dashed line is the output of a moving-average filter (MAF) used to smooth the estimative. It can be noted that transient time does not increase significantly when using the MAF.

Since the noise is a random signal, every simulation will result in a particular estimation curve that has the average amplitude tending towards V_M (or, equivalently, 1p.u.). An important analysis is performed by obtaining the relation between the error of estimated amplitude versus the SNR. This is achieves by making several simulations for each value of SNR. The result is shown in Fig. 9.

Comparing with results obtained in [2], it can be seen that the proposed method presents practically the same performance. While the error in [2] for SNR=10dB is 4%, here the error for this value of SNR is close to 5% for the EPLL output and 3.5% for the AMF output. However the convergence time in our simulations remains about 5 cycles.

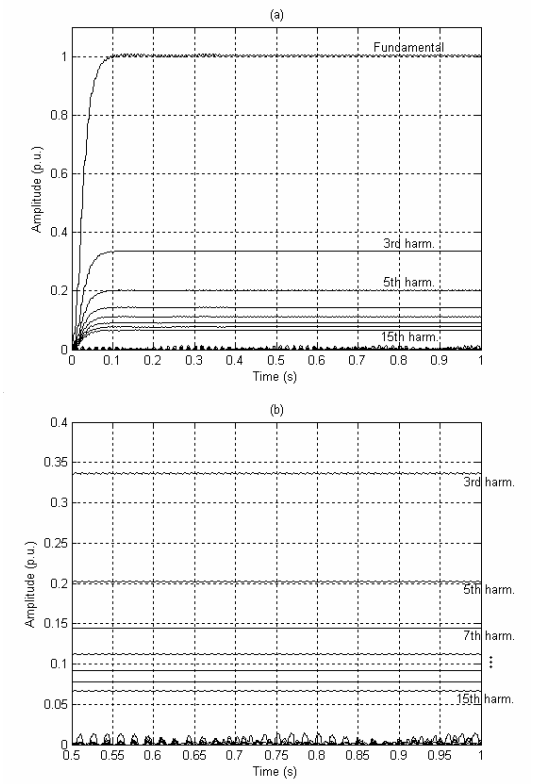

Fig. 7. Amplitude estimation for a signal corrupted with harmonics (a) Total time simulation; (b) zoom at the steady state harmonic estimation

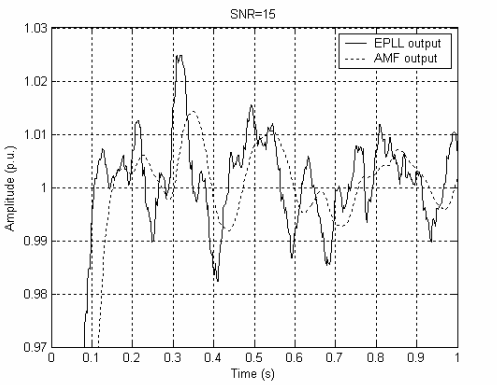

Fig. 8. Example of amplitude estimation for a signal corrupted with noise. A moving average filter is used to improve estimation reducing the error

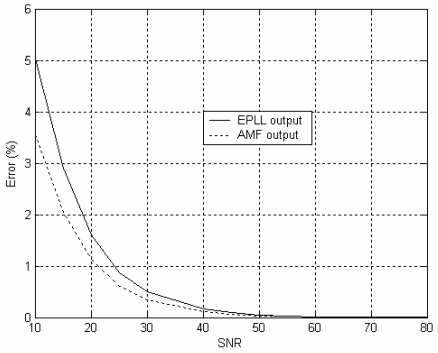

Fig. 9. Relationship between Amplitude Error and SNR

C. Disturbance in amplitude

An important situation for which the system must be tested occurs when the amplitude of the signal varies. Here the signal is assumed to be composed by fundamental, odd harmonics and White Gaussian noise (SNR=40dB),

$$x(t) = V_M \sin(\omega_0 t) + \sum_{\substack{k=3 \\ odd}}^{15} \frac{1}{k} V_M \sin(k\omega_0 t) + n(t) \qquad (9)$$

The total time simulated is 1.0 s. At 0.5 s the amplitude of the signal is reduced to 4/5. Fig. 10 shows the amplitude estimation curves. The transitory response due to decrease in amplitude extinguish in about 5 cycles as well as the transitory response of the beginning of simulation. The error observed in the simulations was less than 1% for the fundamental component and it increases for the high order components reaching nearly 2%.

D. Presence of inter-harmonic

This case discusses the system behavior when an inter-harmonic is added to the fundamental component,

$$x(t) = V_M \sin(\omega_0 t) + \frac{1}{k} V_M \sin(k\delta\omega_0 t) \qquad (10)$$

The parameter δ is the frequency deviation of the k^{th} component. Fig. 11 shows the estimated frequency for δ=1.15 and k=3, which correspond an inter-harmonic added to fundamental of 207Hz.

Basically, there was a slight increase in the transitory response, but with 9 cycles the frequency estimated value is within the error band of 2%. It was observed a slight increase to the transitory response of estimated amplitude too. This is due to the adaptive characteristic of the filter.

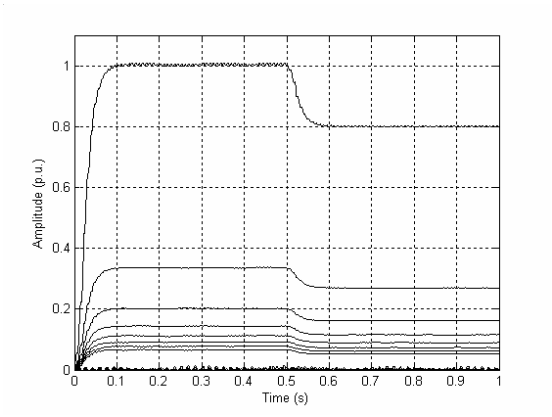

Fig. 10. Performance of the system for a step change in amplitude of input signal

E. Disturbance in frequency

This case deals with change in the frequency of the input signal, that is:

$$x(t) = \sum_{\substack{k=1 \\ odd}}^{15} \frac{1}{k} V_M \sin(k\omega_0(t)) + n(t) \qquad (11)$$

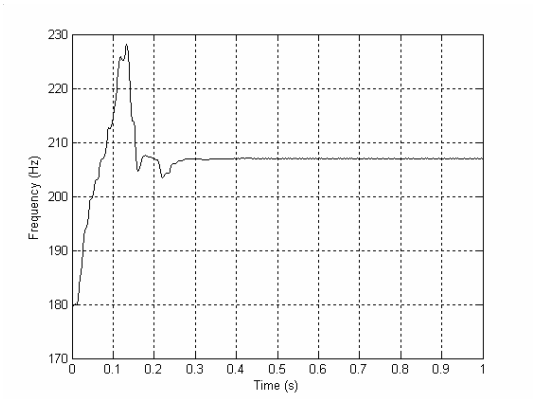

Fig. 11. Frequency tracking of an inter-harmonic component

The total duration of the simulation is 2.0 s. At 1.0 s the fundamental frequency jumps to 61 Hz. This implies the k^{th} harmonic frequency is shifted to $f_k = k \cdot 60 + k$. Fig. 12 presents results for this environment. Fig. 12(a) shows the frequency deviation (k) for each harmonic while Fig. 12(b) shows the effect of a step change in frequency on the amplitude estimation. From Fig. 12(a) it can be seen that transitory response of frequency estimation remains practically at about 5 or 6 cycles, considering a 2% band error. This response is faster than that related in [3].

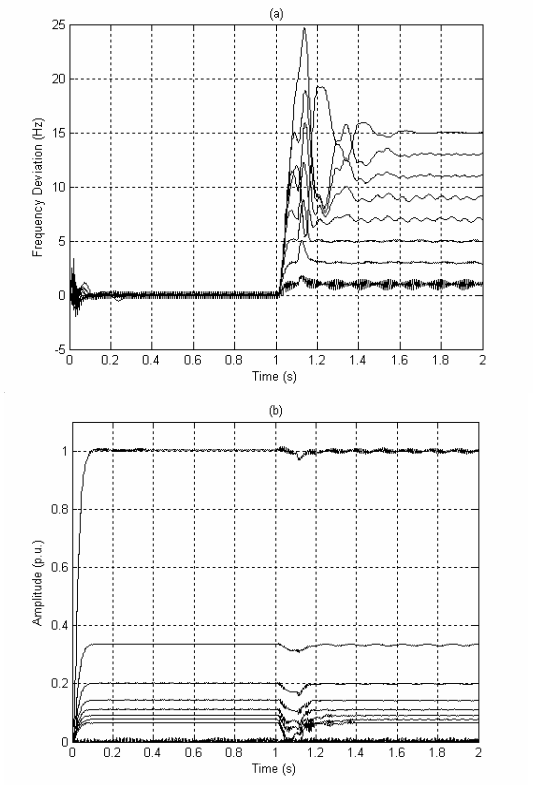

Fig. 12. Frequency tracking for a step change of 1 Hz in fundamental frequency (a) Frequency deviation, (b) Amplitude estimation

F. Flicker

Finally, this case deals with voltage fluctuations, that is, the disturbance referred as Flicker,

$$x(t) = V_M\left[1 + 0.05\sin(2\pi)\right]\sin(\omega_0 t) + n(t) \qquad (12)$$

Equation (11) shows that amplitude of input signal varies with a sinusoidal frequency of 1Hz and the maximum amplitude is 5% of fundamental amplitude. This signal is plotted in Fig. 13(a). Fig. 13(b) presents the behavior of estimator. It can be seen that variations on amplitude are detected, with a very small delay. Moreover, estimated frequency is not affected significantly.

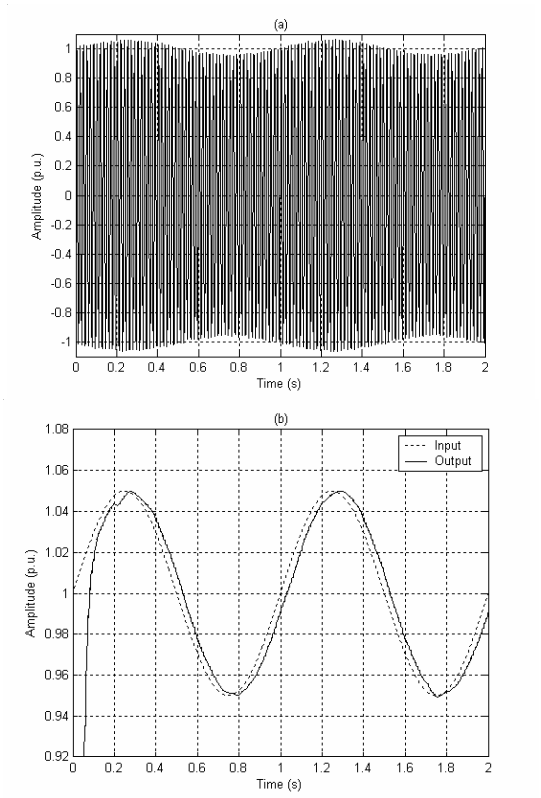

Fig. 13. Response of the method for a voltage fluctuation (Flicker) environment (a) Input signal, (b) Estimated Amplitude

G. Comparative computational effort

The computational effort between the new approach and the approach presented in [3] (single rate) is compared in terms of number of multiplication, addition and table search (functions sin and cos). The total operation number for processing one cycle, i.e. 128 samples, is presented in Table II. To obtain these numbers is necessary take into account the down sampling factor used in Table I and the number of operation in the band-pass filter and EPLL estimator. Note that the computational effort for the multirate approach is greater than the approach of [3] only for the number of adds. However, the multirate approach needs only 82% of multiplies and 7% of table search required for the approach of [3]. It is important to highlight that the EPLL analyzed in this work did not include the extras filters as proposed in [3] to smooth the estimates. If these filters were included the computed data in Table II would be still more favorable to the propose method.

TABLE II
NUMBER OF OPERATIONS REALIZED WITHIN ONE CYCLE OF FUNDAMENTAL TO ESTIMATE UNTIL 15TH HARMONIC

	Adds	**Multiplies**	**Table Search**
Single Rate	9600	15360	3840
Multirate	14125	12616	274

VI. CONCLUSIONS

This paper presents an improved structure of PLL based harmonic estimation [9]. It has been shown that parameters of a high order harmonic can be extracted performing an undersampling of this high frequency signal. The frequency estimated is an apparent frequency that can be converted to its actual value using algebraic relations. The simulations results have shown that the increase in transitory response was not significant. The computational effort is reduced compared with [3] and previous structure [9]. Finally, the fact that PLL estimates an apparent frequency, lower than 240 Hz, makes the implementation in a fixed point DSP-based system more robust.

VII. REFERENCES

[1] M. Karimi-Ghartemani and M. R. Iravani, "A Nonlinear Adaptive Filter for Online Signal Analysis in Power Systems: Applications," *IEEE Trans. on Power Delivery*, vol. 17, no. 2, pp.617-622, Apr. 2002.

[2] M. Karimi-Ghartemani and M. R. Iravani, "Robust and frequency-adaptive measurement of peak value," *IEEE Transactions on PowerDelivery*, vol. 19, no. 2, pp. 481–489, Apr. 2004.

[3] M. Karimi-Ghartemani and M. R. Iravani, "Measurement of harmonics/inter-harmonics of time-varying frequencies," *IEEE Transactions on Power Delivery*, vol. 20, no. 1, pp. 23–31, Jan. 2005.

[4] Y. Baghzouz, R. F. Burch, A. Capasso, A. Cavallini, A. E. Emanuel, M. Halpin, A. Imece, A. Ludbrook, G. Montanari, K. J. Olejniczak, P. Ribeiro, S. Rios-Marcuello, L. Tang, R. Thaliam, and P. Verde, "Time-varying harmonics: Part I—Characterizing measured data," *IEEE Transactions on Power Delivery*,, vol. 13, pp. 938–944, Jul. 1998.

[5] M. V. Chilukuri and P. K. Dash, "Multiresolution S-transform-based fuzzy recognition system for power quality events," *IEEE Transactions on Power Delivery*, vol. 19, no. 1, pp. 323–329, Jan. 2004.

[6] IEC standard draft 61000-4-7: General guide on harmonics and inter-harmonics measurements, for power supply systems and equipment connected thereto, Ed. 2000.

[7] D. Gallo, R. Langella and A. Testa, **"**Desynchronized Processing technique for Harmonic and interharmonic analysis", *IEEE Trans. Power Del.*, vol. 19, pp. 993 – 1001, July 2004.

[8] L. L. Lai, C. T. Tse, W. L. Chan, and A. T. P. So, "Real-time frequency and harmonic evaluation using artificial neural networks," *IEEE Trans.Power Del.*, vol. 14, pp. 52–59, Jan. 1999.

[9] J. R. Carvalho, P. H. Gomes, C. A. Duque, M. V. Ribeiro, A. S. Cerqueira, and J. Szczupak, "PLL based harmonic estimation," *Accepted for publication in IEEE PES conference*, Tampa, Florida-USA, 2007

[10] P. P. Vaidyanathan, *Multirate Systems and Filter Bank*, Englewood Cliffs, New Jersey: Prentice Hall, 1993, pp. 113, 151-157

[11] S. K. Mitra, *Digital Signal Processing: A Computer-based Approach*, McGraw-Hill, 3rd ed., 2006, pp. 383-385, 177, 740